

PACS numbers: 62.20.Qp, 62.23.Hj, 68.37.Hk, 68.37.Lp, 81.20.Hy, 81.40.Jj, 83.50.Uv

Investigation of Properties' Change of Copper Wire in the Process of Twisting and Subsequent Drawing

A. V. Volokitin, I. E. Volokitina, and T. D. Fedorova

*Karaganda Industrial University,
30, Republic Ave.,
101400 Temirtau, Kazakhstan*

In this paper, the change in the mechanical properties of copper wire in the process of deformation in a new way is studied. This new method consists in combining two technologies in one line, namely, traditional drawing and twisting in an equal-channel stepped matrix. The twisting of the work piece occurs precisely in an equal-channel stepped matrix due to its rotation around the work piece axis that allows achieving the twisting in the entire volume of the work piece, followed by calibration of the cross-section due to the passage of the die channel. A physical experiment has shown the possibility of obtaining increased mechanical properties in copper wire by obtaining the nanostructure in the surface layer. In this regard, the use of an improved drawing method, combining torsion methods, which implement a simple shear scheme and the classical drawing process through a die, allows expanding the limits of the use of traditional structural materials.

У цій роботі досліджено зміну механічних властивостей мідного дроту в процесі деформування новим способом. Цей новий метод полягає в поєднанні двох технологій в одній лінії: традиційного волочіння та скручування у рівноканальній ступінчастій матриці. Скручування заготовки відбувається саме в рівноканальній ступінчастій матриці завдяки її обертанню навколо осі заготовки, що дає змогу досягти скручування у всьому об'ємі заготовки з подальшим калібруванням поперечного перерізу за рахунок проходження каналу матриці. Фізичний експеримент показав можливість одержання підвищених механічних властивостей мідного дроту шляхом одержання наноструктури у поверхневому шарі. Тому використання вдосконаленого методу волочіння, що поєднує методи кручення, якими реалізується проста схема зсуву, та класичний процес волочіння через матрицю, уможливорює розширити межі використання традиційних конструкційних матеріалів.

Key words: copper wire, drawing, twisting, microstructure, mechanical

properties.

Ключові слова: мідний дріт, волочіння, скручування, мікроструктура, механічні властивості.

(Received 24 June, 2024; in revised form, 26 June, 2024)

1. INTRODUCTION

Over the past few years, articles on the application of severe plastic deformation (SPD) methods have been the most widely read and cited. This is due to the fact that SPD is successfully used to produce submicron granular structures, and in some cases nanoscale crystallites, in a wide range of alloys [1–7]. However, despite the large number of SPD methods, the creation of deformation nanostructuring technologies for industrial use and, in particular, for the production of mass products, including wire, is a complex scientific and technical problem, the solution of which requires the development of continuous SPD schemes that ensure the production of ultrafine-grained and nanostructures in long metal semi-finished products. Such new technologies can be based on the well-known metal drawing process.

Traditionally, most metals and alloys for structural purposes are characterized by a homogeneous microstructure, where the average grain sizes in different parts are more or less uniform. According to the classical Hall–Petch ratio [8], a homogeneous polycrystalline metal can be strengthened by reducing the average grain size, since an increase in the volume fraction of grain boundaries will further hinder the movement of dislocations. However, a reduction in grain size will inevitably lead to a decrease in the ductility and deformability of the material due to the limited mobility of dislocations, thereby creating a dilemma known as the ‘strength–ductility compromise’, which limits the use of many metallic materials. However, in recent years, metals with a gradient nanostructure have become a new class of structural materials with a promising potential to overcome the compromise between strength and ductility. In such materials, nanostructures smaller than 1000 nm are formed in the surface layer, thereby, improving their mechanical properties [9–11].

Therefore, the development and development of new processes for obtaining high-strength materials with improved strength properties is an urgent and important issue for the development of production. In this regard, the use of an improved drawing method, combining torsion methods, which implement a simple shear scheme and the classical drawing process through a die, allows expanding

the limits of the use of traditional structural materials.

The purpose of this work is to study changes in the mechanical properties of copper wire during deformation in a new way, which consists in twisting the wire in an equal-channel step matrix and traditional drawing.

2. EXPERIMENTAL METHODS

To implement the combined technology for the deformation of copper wire, an industrial drum drawing mill B-1/550M was used. The deformation was carried out at room temperature using the Vs route (the rotation of the wire after each deformation cycle was carried out at 90°). The number of passes was 3. The reduction in the diameter of the wire after each deformation cycle was 0.5 mm. So, after 3 deformation passes, we got a wire with a diameter of 5.0 mm.

The technology of the twisting process in an equal-channel step matrix with subsequent drawing has no significant differences from classical drawing (Fig. 1). At the first stage, the wire is sharpened on the cutting machine to the required diameter. Next, the wire is passed through a lubricated chamber, in which a rotation mechanism is installed. The wire passes through the hole of the matrix bandage, and then through the hole of the die. The front end of the wire is fixed in the pliers of the drawing drum. Next, two segments of an equal-channel stepped matrix are installed around the wire and are inserted into the bandage according to the wedge principle. At this stage, all preparatory operations are completed. After that,

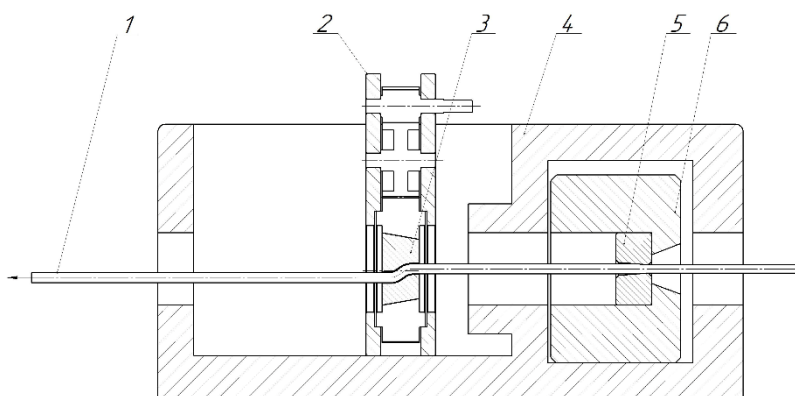


Fig. 1. Diagram of the combined wire deformation process: 1—wire; 2—frame; 3—drawing block; 4—drive gear; 5—intermediate gear; 6—bandage; 7—equal-channel stepped matrix; 8—fiber holder; 9—die.

the mill is started with the output to the planned drawing speed and the mechanism that rotates the equal-channel step matrix is set in motion in parallel.

Metallographic analysis was carried out on a transmission electron microscope JEM 2100. Objects for TEM were prepared by jet polishing on a Tenupol-3 device at room temperature and a voltage of 25 V in a 7% -solution of H_3PO_4 in distilled water.

The effectiveness of hardening after deformation was evaluated by measuring microhardness in accordance with GOST 9450-76 with an interval of 1 mm, as shown in Fig. 2, using the Vickers method. The indenter was a diamond tip in the form of a four-sided pyramid with a square base. The load was of 0.5 N.

Tensile tests were carried out using the Instron 5982 electromechanical measuring machine. The tests were carried out in accordance with GOST 10446-80 'Wire. Tensile testing method' and GOST 1497-2000 'Metals. The method of tensile testing'. These standards establish methods for testing static tensile strength at a temperature of 20°C of wire made of metals and their alloys with a diameter or maximum cross-sectional size not exceeding 16 mm of circular cross-section. As test samples, wire segments with an initial estimated working length of 26 ± 0.1 mm and a diameter of 5 mm, limited with an error of up to 1%, were used. To recalculate the elongation with the reference of the rupture site to the middle of the calculated length, marks were scratched along the entire working length of the sample at regular intervals. The full length of the sample included sections for fixing it in the clamps of the bursting machine. The strain rate was of $0.56 \cdot 10^{-3} s^{-1}$, which corresponds to a stretching rate of 0.5 mm/min. After the tensile tests, a fractographic analysis of the surface of the destroyed samples was carried out using scanning electron microscopy (SEM). Due to the large depth of focus, SEM gives an apparent volume and thereby facilitates the interpretation of the fracture topography.

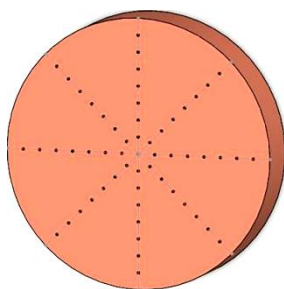


Fig. 2. Hardness measurement point diagrams.

3. RESULTS AND DISCUSSION

Figure 3 shows photos of the microstructure obtained using TEM. The first image was obtained at a distance of ≈ 0.2 mm from the surface of the wire (surface layer) (Fig. 3, *a*). As shown, the grain boundaries are fibrous and curved, which is usually characteristic of a large number of defects, the average grain size is 500 nm. This approach to the formation of the nanostructure of the wire surface layer is created due to friction and torsion during twisting in an equal-channel stepped matrix and is based on the use of the strain-rate intensity coefficient, which controls the thickness of the layer of intense plastic deformation. As a result, a layer of nanofine-deformed grains is created in the wire with generated at the material-tool contact. The following TEM image was obtained at a distance of ≈ 2 mm from the wire surface (middle layer) (Fig. 3, *b*). A bimodal structure has been formed here, which consists of small grains with high-angle boundaries and large grains with a developed substructure. The average grain size is 2 microns. Inside the grains, a thin structure is formed in the form of clusters of dislocations and cells. Large grains were most likely formed by the mechanism of diffusion-free recrystallization, since, if dynamic recrystallization had occurred, the grains would not have had distortions of the crystal lattice and would not contain defects. In addition, the last image was obtained from the central part of the wire. The structure is a cellular dislocation structure of deformation origin with an average grain size of 4 microns (Fig. 3, *c*). They are observed as large grains with a small number of subboundaries, as well as grains containing a large number of subboundaries.

Figure 4 shows the stress-strain curves and mechanical properties of the samples obtained during stretching. The tensile strength of deformed copper wire compared to undeformed increases from

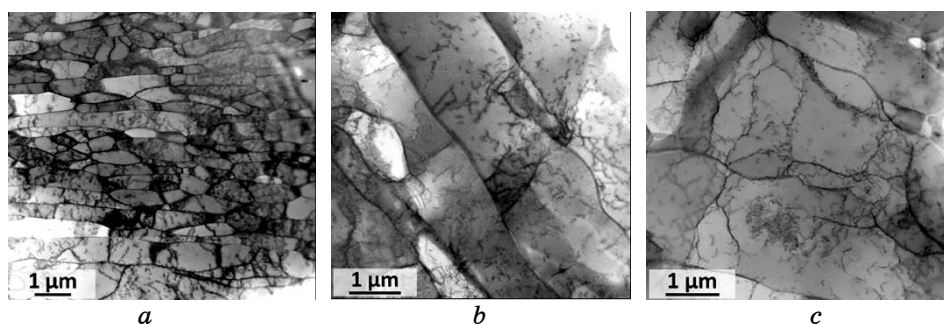


Fig. 3. Microstructure of deformed copper wire (cross section): *a*—surface layer; *b*—middle layer; *c*—central part.

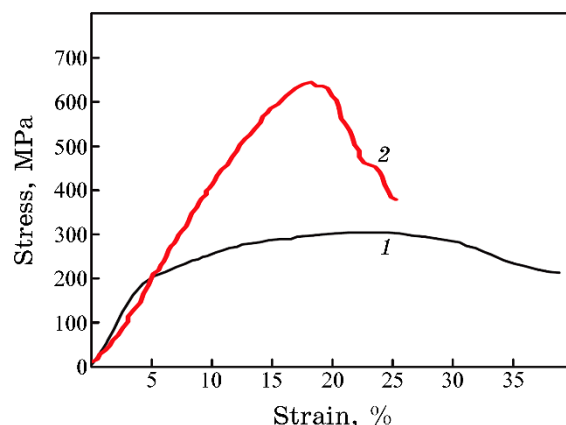


Fig. 4. Stretching curves of copper wire: 1—before deformation; 2—after 3 deformation cycles.

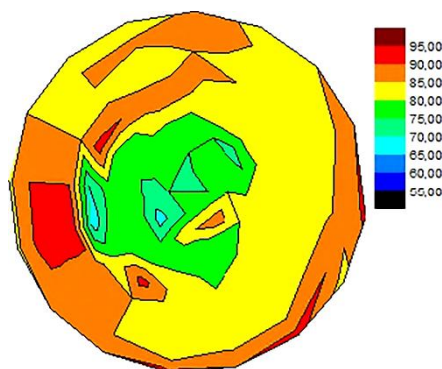


Fig. 5. Hardness distribution map in copper wire in cross section.

302 to 635 MPa, and the yield strength increases from 196 to 406 MPa—an increase of almost 100%. The elongation decreased from 42% to 27%. The obtained results of plastic properties are superior to some existing SPD methods of wire [12–15].

Figure 5 demonstrates a map of the hardness distribution of the sample, which shows that the hardness values of the surface layers are higher. The central regions have lower hardness values. This hardness distribution confirms the presence of a gradient microstructure.

A more accurate measurement of microhardness was carried out by Vickers hardness test randomly. Thus, the average value of microhardness in the surface layers was of 216 MPa, in the middle layers microhardness value was of 174 MPa, and 155 MPa in the centre of the wire. Such a spread of microhardness can be explained

by the formation of a gradient structure and the hardening of grain boundaries due to an increase in the density of dislocations.

Fractographic analysis of copper wire after stretching showed that the fracture has a mixed viscous character. The destruction zone of the wire surface layer has elongated pits and micropores; there are no cut zones. This indicates viscous destruction, since the main feature of such destruction is high-energy intensity, and slow crack development, resulting in a large number of pits. The middle part of the wire occupies the periphery of the fracture and consists of ridges of separation, the microrelief is stepped and traces of viscous stratification are visible. In the central part of the copper wire, together with large sections of the quasi-cut, areas with the formation of a shallow relief are observed.

4. CONCLUSION

Metallographic analysis showed the presence of a gradient structure in the copper wire after deformation by a new method. A nanostructure with a grain size of ≈ 500 nm was obtained in the surface layer, which increases to 4 microns towards the centre of the wire. The micromechanical tests carried out to determine the microhardness confirmed the presence of a gradient microstructure in the copper wire. Tensile tests showed not only a 2-fold increase in the strength properties of the wire, but not a strong decrease in plastic properties. Fractographic analysis of the destroyed wire samples showed the presence of a viscous fracture, which also indicates good plastic properties.

ACKNOWLEDGMENT

This research has been/was/is funded by the Science Committee of the Ministry of Science and Higher Education of the Republic of Kazakhstan (Grant No. AP19676903).

REFERENCES

1. I. E. Volokitina, *Progress in Physics of Metals*, **24**, No. 3: 593 (2023); <https://doi.org/10.15407/ufm.24.03.593>
2. A. Bychkov and A. Kolesnikov, *Metallography, Microstructure, and Analysis*, **12**, No. 3: 564 (2023); <https://doi.org/10.1007/s13632-023-00966-y>
3. M. A. Latypova, V. V. Chigirinsky, and A. S. Kolesnikov, *Progress in Physics of Metals*, **24**, No. 1: 132 (2023); <https://doi.org/10.15407/ufm.24.01.132>
4. A. Denissova, T. Fedorova, D. Lawrinuk, A. Kolesnikov, A. Yerzhanov, Y. Kuatbay, and Y. Liseitsev, *Case Stud. Constr. Mater.*, **18**: e02346 (2023);

- <https://doi.org/10.3390/ma15072584>
5. M. Ved, N. Sakhnenko, I. Yermolenko, and G. Yar-Mukhamedova, *Chemico-Technological Journal*, **8**: 147 (2021); <https://doi.org/10.18321/ectj697>
 6. A. V. Volokitin, I. E. Volokitina, and E. A. Panin, *Progress in Physics of Metals*, **23**: No. 3: 411 (2022); <https://doi.org/10.15407/ufm.23.04.684>
 7. I. Volokitina, A. Volokitin, and D. Kuis, *J. Chem. Technol. Metall.*, **56**: 643–647 (2021).
 8. M. Murugesan, D. Won, and J. Johnson, *Materials*, **12**: 609 (2019); <https://doi.org/10.3390/ma12040609>
 9. I. E. Volokitina, A. V. Volokitin, E. Panin, T. Fedorova, D. Lawrinuk, A. Kolesnikov, A. Yerzhanov, Z. Gelmanova, and Y. Liseitsev, *Case Stud. Constr. Mater.*, **19**: e02609 (2023); <https://doi.org/10.1016/j.cscm.2023.e02609>
 10. M. Latypova, V. Chigirinsky, and A. Kolesnikov, *Progress in Physics of Metals*, **24**, No. 1: 132 (2023); <https://doi.org/10.15407/ufm.24.01.132>
 11. I. E. Volokitina, *Metal Science and Heat Treatment*, **63**, Nos. 3–4: 163 (2021).
 12. L. David, *Journal of The Minerals*, **59**: 21 (2021); <https://doi.org/10.1007/s11837-007-0111-7>
 13. B. Sapargaliyeva, A. Agabekova, G. Ulyeva, A. Yerzhanov, and P. Kozlov, *Case Stud. Constr. Mater.*, **18**: e02162 (2023); <https://doi.org/10.1016/j.cscm.2023.e02162>
 14. G. I. Raab, D. V. Gunderov, L. N. Shafigullin, Yu. M. Podrezov, M. I. Danylenko, N. K. Tsenev, R. N. Bakhtizin, G. N. Aleshin, and A. G. Raab, *Materials Physics and Mechanics*, **3**, No. 24: 242 (2015).
 15. I. E. Volokitina and A. V. Volokitin, *Physics of Metals and Metallography*, **119**, No. 9: 917 (2018).